Journal of Applied Pharmaceutical Science Vol. 0(00), pp 001-008, 2024
Available online at http://www.japsonline.com
DOI: 10.7324/JAPS.2024.158840
ISSN 2231-3354

Cytotoxic constituents of *Cymbidium tracyanum* L.Castle

Nonthalert Lertnitikul[1], Rutt Suttisri[1], Khin Lay Sein[2], Suree Jianmongkol[2], Cherdsak Boonyong[3], Witchuda Thanakijcharoenpath[1]*

[1]Department of Pharmacognosy and Pharmaceutical Botany, Faculty of Pharmaceutical Sciences, Chulalongkorn University, Bangkok, Thailand.
[2]Department of Pharmacology and Physiology, Faculty of Pharmaceutical Sciences, Chulalongkorn University, Bangkok, Thailand.
[3]Pharmacology and Toxicology Unit, Department of Medical Science, Faculty of Science, Rangsit University, Pathum Thani, Thailand.

ARTICLE HISTORY

Received on: 26/06/2023
Accepted on: 10/09/2023
Available Online: XX

Key words:
Cymbidium tracyanum, cymbisamoquinone, phenanthrenequinones, phenanthrenes, bibenzyls, cytotoxic activity.

ABSTRACT

Three phenanthrene derivatives, cymbisamoquinone (**1**), calanquinone B (**6**), and 3,7-dihydroxy-2,4,6-trimethoxyphenanthrene (**2**), and two bibenzyls, tristin (**3**) and gigantol (**4**), together with the lignan (+)-pinoresinol (**5**), were isolated from the whole plants of *Cymbidium tracyanum* L.Castle (Orchidaceae). Their structures were determined through spectroscopic analysis as well as a comparison of the spectral data with literature values. The phytochemical constituents of this plant have been reported for the first time. All isolated compounds were evaluated for *in vitro* cytotoxic activity against human colon (Caco-2) and breast (MCF-7) cancer cell lines, doxorubicin-resistant (MCF-7/DOX) and mitoxantrone-resistant (MCF-7/MX) MCF-7 sublines, together with normal human fibroblast (NIH/3T3) cell line. Among the isolated compounds, **1** exhibited the strongest and relatively selective activity on MCF-7/DOX cells. The results obtained from molecular docking study suggested that the cytotoxicity of **1** on MCF-7/DOX cells was possibly due to induction of apoptosis via suppression of the cell survival systems mediated by the mitogen-activated protein kinases and protein kinase B/glycogen synthase kinase-3β/nuclear factor erythroid 2-related factor 2 signaling pathways.

INTRODUCTION

The genus *Cymbidium* (Orchidaceae) comprises about 80 species of epiphytic, lithophytic, and terrestrial herbs which are widely distributed from tropical and subtropical Asia to northern Australia [1,2]. A variety of these orchids are cultivated as ornamentals, particularly *Cymbidium* hybrids. The roots, leaves, seeds, or whole plants of several species are employed in herbal medicine while the flowers in cosmetics and certain plant parts, such as flower buds and pseudobulbs, as food in some countries [3]. Phytochemical studies on *Cymbidium* plants revealed that their major constituents were derivatives of bibenzyls and phenanthrenes [4–14]. These groups of compounds are structurally and biosynthetically related; their derivatives are mainly found in Orchidaceae, being a characteristic of the family. Various biological activities of these metabolites isolated from orchids have been reported, including cytotoxic, antimicrobial, anti-allergic, anti-inflammatory, and anti-platelet activities [4–10,15–17]. Among these activities, one that has been most extensively studied for bibenzyl/phenanthrene derivatives is cytotoxic activity, and several of them have been found to possess promising effects [15,16,18]. Compounds of interest include 9,10-dihydrophenenthrenes and 3-methoxy-1,4-phenanthrenequinones [15,16]. Previous studies indicated the presence of such structural types in different members of *Cymbidium* [4–13].

Based on chemotaxonomic data, the genus *Cymbidium* is a potential source of bibenzyl/phenanthrene derivatives with interesting cytotoxic activity. However, relatively few species of the genus have been phytochemically investigated. *Cymbidium tracyanum* L.Castle is one of *Cymbidium* species with no previous report on phytoconstituents. It is a large-sized orchid with strongly fragrant flowers, found distributed in China, Myanmar, Thailand, and Vietnam [2]. The objective of this study is to reveal the chemical constituents of this

*Corresponding Author
Witchuda Thanakijcharoenpath, Department of Pharmacognosy and Pharmaceutical Botany, Faculty of Pharmaceutical Sciences, Chulalongkorn University, Bangkok, Thailand.
E-mail: witchuda.t@chula.ac.th

plant, especially bibenzyl/phenanthrene derivatives, together with their cytotoxic activity, providing additional information on this group of compounds which may contribute to further research for anticancer drug development. Six constituents of *C. tracyanum* L.Castle are reported herein; their chemical structures are shown in Figure 1.

MATERIALS AND METHODS

General experimental procedures

Nuclear Magnetic Resonance (^{1}H NMR, ^{13}C-NMR, and 2D-NMR) spectra were recorded on a Bruker Avance Neo 400 MHz NMR spectrometer (Billerica, MA, USA). High-resolution electrospray mass spectra (HR-ESI-MS) were obtained on a Bruker microTOF mass spectrometer. Thin-layer chromatography was performed on precoated silica gel 60 F_{254} plates (Merck, KGaA, Darmstadt, Germany). Column chromatography was carried out using either silica gel 60 (230–400 mesh, Merck) or Sephadex LH-20 (Pharmacia Biotech AB, Uppsala, Sweden).

Plant materials

The whole plants of *C. tracyanum* L.Castle were collected from an orchid farm in San Pa Tong, Chiang Mai, Thailand (18370 51″N 98530 43″E), in August 2020. The plant was identified by Associate professor Rutt Suttisri (Department of Pharmacognosy and Pharmaceutical Botany, Faculty of Pharmaceutical Sciences, Chulalongkorn University). A voucher specimen (RS17021) has been deposited at the Herbarium of the Faculty of Pharmaceutical Sciences, Chulalongkorn University, Bangkok, Thailand.

Extraction and isolation

The fresh whole plants (5.2 kg) of *C. tracyanum* L.Castle were cut into small pieces and dried in a hot-air oven at 50°C. The dried plant material (2.5 kg) was macerated with 95% MeOH (3 × 5 l) at room temperature. The combined extract was evaporated under reduced pressure to yield 64 g of crude MeOH extract which was then dispersed in water and partitioned with EtOAc (3 × 1 l). The obtained EtOAc extract (30 g) was separated on a silica gel column, eluted with a gradient mixture of n-hexane/EtOAc (7:3 to 0:1), into five fractions (A–E). Fraction B (7.5 g) was fractionated on a silica gel column, eluted with *n*-hexane/EtOAc (7:3), into four subfractions (B1–B4). Separation of subfraction B3 (31 mg) on a Sephadex LH-20 column, eluted with MeOH, gave compound **1** (1 mg) and three subfractions (B3/2–B3/4). Further separation of subfraction B3/2 (12 mg) on a Sephadex LH-20 column, eluted with MeOH, afforded compound **2** (3 mg). Fraction C (1.1 g) was fractionated on a silica gel column, eluted with *n*-hexane/EtOAc (7:3), into three subfractions (C1–C3). Separation of subfraction C2 (0.7 g) on a Sephadex LH-20 column, eluted with MeOH, gave three subfractions (C2/1–C2/3). Further separation of subfraction C2/2 (0.3 g) on a Sephadex LH-20 column, eluted with MeOH, afforded compound **3** (38 mg). Fraction D (0.9 g) was fractionated on a silica gel column, eluted with a gradient mixture of CH_2Cl_2/acetone (9:1 to 0:1), into three subfractions (D1–D3). Separation of subfraction D1 (0.3 g) on a silica gel column, eluted with CH_2Cl_2, afforded compound **4** (1 mg), and that of D2 (0.4 g) on a silica gel column, eluted with a gradient mixture of CH_2Cl_2/acetone (9:2 to 0:1), afforded compounds **5** (4 mg) and **6** (4 mg).

Cymbisamoquinone (1): red amorphous powder, positive HR-ESI-MS *m/z* 285.0765 $[M+H]^+$ (calcd for $C_{16}H_{13}O_5$, 285.0763). ^{1}H-NMR (400 MHz, $CDCl_3$) δ_H ppm: 7.96 (1H, *d*, *J* = 8.4 Hz, H-10), 7.90 (1H, *d*, *J* = 8.4 Hz, H-9), 7.08 (1H, *d*, *J* = 10.2 Hz, H-3), 7.00 (1H, *s*, H-8), 6.84 (1H, *d*, *J* = 10.2 Hz, H-2), 6.22 (1H, *br s*, 6-OH), 4.07 (3H, *s*, 7-OCH_3), and 3.92 (3H, *s*, 5-OCH_3). ^{13}C-NMR (100 MHz, $CDCl_3$), δ_C ppm: 186.2 (C-4), 185.1 (C-1), 150.5 (C-7), 142.0 (C-5), 140.8 (C-6), 140.4 (C-3), 135.3 (C-2), 132.4 (C-8a), 132.3 (C-9), 131.7 (C-4a), 131.2 (C-10a), 120.3 (C-10), 119.5 (C-4b), 102.5 (C-8), 60.5 (5-OCH_3), and 56.3 (7-OCH_3). ^{1}H-NMR (400 MHz, acetone-d_6) δ_H ppm: 8.45 (1H, *br s*, 6-OH), 8.04 (1H, *d*, *J* = 8.4 Hz, H-9), 7.85 (1H, *d*, *J* = 8.4 Hz, H-10), 7.29 (1H, *s*, H-8), 7.14 (1H, *d*, *J* = 10.2 Hz, H-3), 6.86 (1H, *d*, *J* = 10.2 Hz, H-2), 4.06 (3H, *s*, 7-OCH_3), and 3.95 (3H, *s*, 5-OCH_3). ^{13}C-NMR (100 MHz, acetone-d_6), δ_C ppm: 187.1 (C-4), 185.5 (C-1), 152.7 (C-7), 143.5 (C-5), 142.5 (C-6), 141.5 (C-3), 136.1 (C-2), 133.2 (C-8a), 133.2 (C-4a), 132.9 (C-9), 131.8 (C-10a), 121.0 (C-4b), 120.2 (C-10), 103.4 (C-8), 60.4 (5-OCH_3), and 56.7 (7-OCH_3).

3,7-Dihydroxy-2,4,6-trimethoxyphenanthrene (2): brown amorphous powder, positive HR-ESI-MS *m/z* 323.0893 $[M+Na]^+$ (calcd for $C_{17}H_{16}O_5Na$ 323.0895). ^{1}H-NMR (400 MHz, $CDCl_3$) δ_H ppm: 8.99 (1H, *s*, H-5), 7.48 (2H, *s*, H-9/H-10), 7.23 (1H, *s*, H-8), 7.06 (1H, *s*, H-1), 6.00* (1H, br *s*, 7-OH), 5.97* (1H, br *s*, 3-OH), 4.08 (3H, *s*, 6-OCH_3), 4.04 (3H, *s*, 2-OCH_3), and 3.97 (3H, *s*, 4-OCH_3) *interchangeable. ^{13}C-NMR (100 MHz, $CDCl_3$), δ_C ppm: 146.6 (C-2/C-6), 144.7 (C-7), 143.5 (C-4), 138.7 (C-3), 127.9 (C-8a), 126.2 (C-10a), 125.0 (C-10), 124.8 (C-9), 123.4 (C-4b), 118.6 (C-4a), 111.0 (C-8), 106.7 (C-5), 104.7 (C-1), 60.0 (4-OCH_3), 56.0 (2-OCH_3), and 55.9 (6-OCH_3).

Tristin (3): brown amorphous powder, positive HR-ESI-MS *m/z* 283.0946 $[M+Na]^+$ (calcd for $C_{15}H_{16}O_4Na$ 283.0946). ^{1}H-NMR (400 MHz, $CDCl_3$) δ_H ppm: 6.83 (1H, *d*, *J* = 8.0 Hz, H-5), 6.67 (1H, *dd*, *J* = 8.0, 1.8 Hz, H-6), 6.61 (1H, *d*, *J* = 1.8 Hz, H-2), 6.22 (2H, *d*, *J* = 2.1 Hz, H-2′/H-6′), 6.19 (1H, *t*, *J* = 2.1 Hz, H-4′), 5.48 (1H, *br s*, 4-OH), 4.86 (2H, *br s*, 3′-OH/5′-OH), 3.84 (3H, *s*, 3-OCH_3), and 2.80 (4H, *m*, H-α/H-β). ^{13}C-NMR (100 MHz, $CDCl_3$), δ_C ppm: 156.7 (C-3′/C-5′), 146.3 (C-3), 144.9 (C-1′), 143.8 (C-4), 133.5 (C-1), 121.0 (C-6), 114.2 (C-5), 111.1 (C-2), 108.2 (C-2′/C-6′), 100.4 (C-4′), 55.9 (3-OCH_3), 38.1 (C-β), and 37.2 (C-α).

Gigantol (4): brown amorphous powder, positive HR-ESI-MS *m/z* 275.1284 $[M+H]^+$ (calcd for $C_{16}H_{19}O_4$, 275.1283). ^{1}H-NMR (400 MHz, $CDCl_3$) δ_H ppm: 6.82 (1H, *d*, *J* = 8.0 Hz, H-5), 6.68 (1H, *dd*, *J* = 8.0, 2.0 Hz, H-6), 6.62 (1H, *d*, *J* = 2.0 Hz, H-2), 6.35 (1H, *t*, *J* = 1.4 Hz, H-4′), 6.24 (2H, *t*, *J* = 1.4 Hz, H-2′/H-6′), 5.47* (1H, *br s*, 4-OH), 4.80* (1H, *br s*, 3′-OH), 3.84 (3H, *s*, 3-OCH_3), 3.75 (3H, *s*, 5′-OCH_3), and 2.82 (4H, *m*, H-α/H-β) *interchangeable.

(+)-Pinoresinol (5): brown amorphous powder, positive HR-ESI-MS *m/z* 357.1433 $[M+H]^+$ (calcd for $C_{20}H_{21}O_6$, 357.1338). ^{1}H-NMR (400 MHz, $CDCl_3$) δ_H ppm: 6.90 (2H, *d*, *J* = 1.6 Hz, H-2/H-2′), 6.86 (2H, *d*, *J* = 7.4 Hz, H-5/H-5′), 6.82 (2H, *dd*, *J* = 7.4, 1.6 Hz, H-6/H-6′), 5.59 (2H, *br s*, 4-OH/4′-OH), 4.74 (2H, *d*, *J* = 4.4 Hz, H-7/H-7′), 4.24 (2H,

m, H-9a/H-9′a), 3.90 (6H, *s*, 3-OCH_3/3′-OCH_3), 3.88 (2H, *m*, H-9b/H-9′b), and 3.10 (2H, *m*, H-8/H-8′). ^{13}C-NMR (100 MHz, $CDCl_3$), δ_C ppm: 146.7 (C-3/C-3′), 145.2 (C-4/C-4′), 132.9 (C-1/C-1′), 119.0 (C-6/C-6′), 114.2 (C-5/C-5′), 108.6 (C-2/C-2′), 85.9 (C-7/C-7′), 71.7 (C-9/C-9′), 55.6 (3-OCH_3/3′-OCH_3), and 54.2 (C-8/C-8′).

Calanquinone B (6): red amorphous powder, positive HR-ESI-MS *m/z* 315.0866 $[M + H]^+$ (calcd for $C_{17}H_{15}O_6$ 315.0869). ^{1}H-NMR (400 MHz, $CDCl_3$) δ_H ppm: 7.97 (1H, *d*, *J* = 8.4 Hz, H-10), 7.90 (1H, *d*, *J* = 8.4 Hz, H-9), 6.99 (1H, *s*, H-8), 6.21 (1H, *br s*, 6-OH), 6.04 (1H, *s*, H-2), 4.07 (3H, *s*, 7-OCH_3), 3.98 (3H, *s*, 5-OCH_3), and 3.95 (3H, *s*, 3-OCH_3). ^{13}C-NMR (100 MHz, $CDCl_3$), δ_C ppm: 184.9 (C-1), 181.4 (C-4), 162.9 (C-3), 150.2 (C-7), 141.9 (C-5), 140.8 (C-6), 132.8 (C-9), 132.0 (C-8a), 131.7 (C-10), 130.6 (C-4a), 120.2 (C-10), 119.8 (C-4b), 106.4 (C-2), 102.4 (C-8), 60.4 (7-OCH_3), 56.6 (3-OCH_3), and 56.4 (5-OCH_3).

Cytotoxicity assay

Human colon cancer (Caco-2), breast cancer (MCF-7), and normal fibroblast (NIH/3T3) cell lines were obtained from the American Type Culture Collection (ATCC, Rockville, MD). Doxorubicin-resistant (MCF-7/DOX) and mitoxantrone-resistant (MCF-7/MX) MCF-7 sublines were developed from the MCF-7 cell line, following the methods described in previous studies [19,20]. Cytotoxic activities of the isolated compounds against these cells were evaluated by 3-(4,5-dimethylthiazolyl)-2,5-diphenyltetrazolium bromide (MTT) assay, using doxorubicin and mitoxantrone as positive controls. The cells were seeded onto 96-well microplates at the density of 5×10^3 cells/well and cultured for 24 hours. Then, they were incubated with different concentrations of the tested compounds at 37°C for 72 hours. After treatment, the cells were washed and further incubated in a serum-free medium containing 0.83 mg/ml MTT solution for 3 hours. The formazan crystals in these cells were dissolved with dimethyl sulfoxide and the absorbance was measured at 570 nm with a microplate reader [21]. IC_{50} values were determined from the dose-response curves based on three independent experiments (*N* = 3), each of which was performed in triplicate (*n* = 3). The selectivity index (SI) was calculated as the ratio of the IC_{50} value for the normal cells (NIH/3T3) to that for the cancer cells.

Molecular docking study

The 3-D structure of compound **1** was drawn by using Chem3D version 16.0 (PerkinElmer, Waltham, MA). The protein data bank (PDB) files of macromolecules including mitogen-activated proteins [MAPKs; ERK-2 (4QTA), JNK (1PMN), and p-38 (5MI5)], protein kinase B/glycogen synthase kinase-3β/nuclear factor erythroid 2-related factor 2 (Akt/GSK-3β/Nrf-2) [Akt (3O96)/GSK-3β (5K5N)/Nrf-2 (4IQK)] and detoxification proteins [hemoxygenase-1:HO-1 (3HOK) and NAD(P)H quinone dehydrogenase 1:NQO-1 (2F1O)] were downloaded from RCSB protein data bank. The respective files were selected based on the homology with human homologous proteins. These PDB files, representing protein structures similar to those of humans, were used to validate and evaluate the mechanism of small molecule inhibitors in published studies. The docking of the ligand for the protein structure was evaluated in PDBQT (Protein Data Bank, Partial Charge (Q), & Atom Type (T)) files by using AutoDoc Suite 4.2.6 (TSRI, La Jolla, CA). The dimensions of a grid box, set for the target site of proteins were 60 Å × 60 Å × 60 Å. The lowest binding energy (ΔG) and inhibition constant (Ki) were observed. The protein-ligand interactions were visualized in 2-D and 3-D by using Discovery Studio 2021 Client (BIOVIA, San Diego, CA).

All target proteins were prepared for docking by removal of the co-crystallized ligand and additional water molecules; hydrogen ions and gasteiger charges were then added. Redocking of the ligand (**1**) into the binding pocket, where the co-crystallized ligand was removed, was performed 10 times for each of the target proteins. The best-docked poses were selected and further analyzed by calculating the cluster room mean square deviation (RMSD) value in docking log file. In our experiments, the first range cluster RMSD values for all the protein-ligand complexes were demonstrated to equal zero, suggesting good docking results, as the values were less than 2.0 Å [22].

RESULTS AND DISCUSSION

Compound **1** was obtained as a red amorphous powder. The compound gave the $[M+H]^+$ ion peak at *m/z* 285.0765 (calculated for $C_{16}H_{13}O_5$, 285.0763) in the HR-ESI-MS, corresponding to the molecular formula of $C_{16}H_{12}O_5$. Its ^{1}H-NMR spectrum exhibited two pairs of doublets corresponding to two sets of *ortho*-coupled protons; one appeared at δ_H 7.96 (1H, *d*, *J* = 8.4 Hz, H-10) and 7.90 (1H, *d*, *J* = 8.4 Hz, H-9), and the other at δ_H 7.08 (1H, *d*, *J* = 10.2 Hz, H-3) and 6.84 (1H, *d*, *J* = 10.2 Hz, H-2). The rest of signals were all observed as singlets, including one olefinic singlet at δ_H 7.00 (1H, *s*, H-8)], one hydroxy singlet at δ_H 6.22 (1H, *br s*, 6-OH), and two methoxy singlets at δ_H 4.07 (3H, *s*, 7-OCH_3) and 3.92 (3H, *s*, 5-OCH_3). In ^{13}C-NMR spectrum, the two most downfield signals at δ_C 186.2 and 185.1 were indicative of two carbonyl groups, and two signals at δ_C 60.5 and 56.3 supported the presence of two methoxy groups. In addition, twelve signals for five methylene and seven methine carbons were observed in the region of 100.0–155.0 ppm. The above information suggested the structure of a trisubstituted 1,4-phenanthrenequinone with one hydroxy and two methoxy groups. In the HMBC (Heteronuclear Multiple Bond Correlation) spectrum (Fig. 2), correlations between the hydroxy group (δ_H 6.22) and both carbons corresponding to the methoxy groups (δ_C 142.0 and δ_C 150.5) were observed, indicating that the three substituents were located at adjacent positions with the hydroxy group being placed in the middle. Hence, the substitutions might be at positions 5, 6, and 7 or 6, 7, and 8 of the phenanthrenequinone structure. The only uncoupled aromatic proton was indicated to be H-8, rather than H-5, by HMBC spectrum which displayed the correlations of this proton (δ_H 7.00, *s*, H-8) with a carbon corresponding to one of *ortho*-coupled protons (δ_C 132.3, C-9) and with two carbons corresponding to the hydroxy group (δ_C 140.8, C-6) and to one of the methoxy groups (δ_C 150.5, C-7). The uncoupled proton H-8 also showed a correlation with this methoxy group (δ_H 4.07, *s*, 7-OCH_3) in the NOESY (Nuclear Overhauser Effect Spectroscopy) spectrum (Fig. 2) while its correlation with the hydroxy group was not observed. Therefore, the three substituents of **1** were assigned to be 5-OCH_3, 6-OH, and 7-OCH_3.

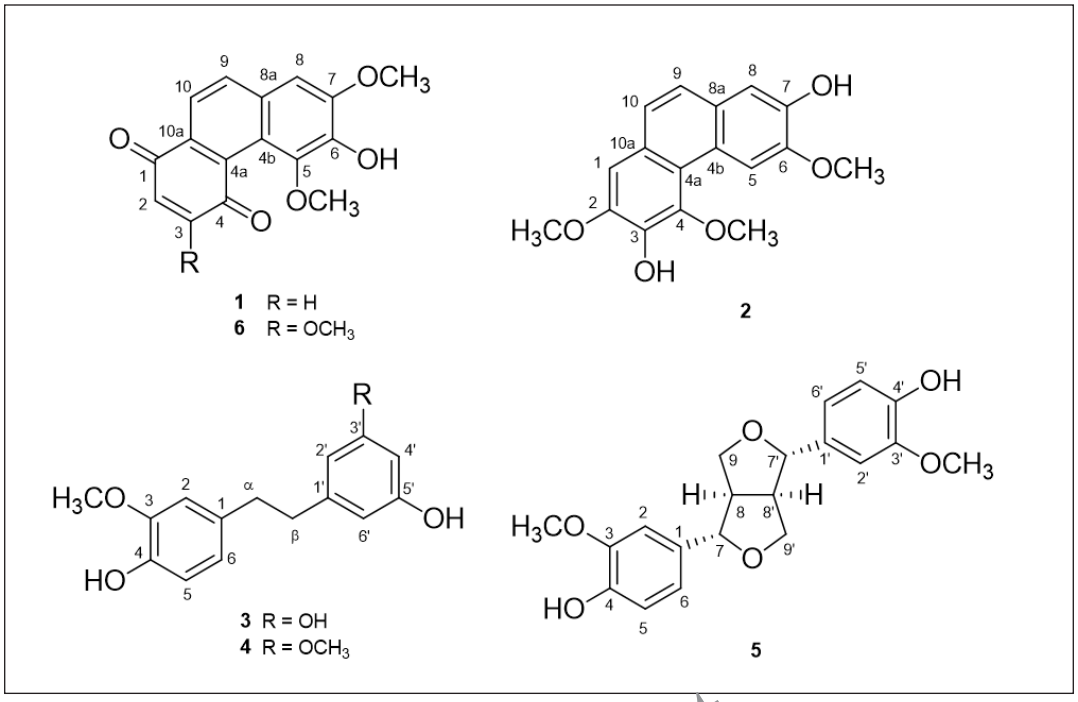

Figure 1. Chemical structures of **1-6.**

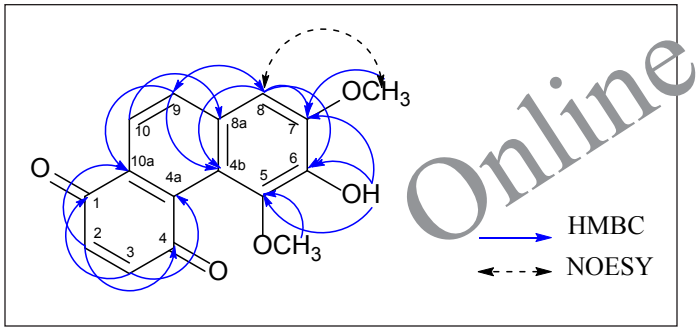

Figure 2. Key HMBC and NOESY correlations of **1.**

The NMR spectra of **1** were also measured in acetone-*d*6, and the resulting NMR data mostly conformed to those obtained in $CDCl_3$. Some differences in the ^{1}H-NMR spectra were notable; these concerned the relative chemical shifts observed for H-9 and H-10, and for H-3 and H-8. In $CDCl_3$ the more downfield signals corresponded to H-10 (H-10, δ_H 7.96; H-9, δ_H 7.90) and H-3 (H-3, δ_H 7.08; H-8, δ_H 7.00) while in acetone-d_6, to H-9 (H-9, δ_H 8.04; H-10, δ_H 7.85) and H-8 (H-8, δ_H 7.29; H-3, δ_H 7.14). In addition, the proton signal of the hydroxy group at C-6 in the two solvents was observed at significantly different chemical shifts (δ_H 6.22 in $CDCl_3$ and δ_H 8.45 in acetone-d_6).

Owing to all the above information, **1** was identified to be cymbisamoquinone (6-hydroxy-5,7-dimethoxy-1,4-phenanthrenequinone) [4]. This phenanthrenequinone was previously isolated from *Cymbidium* plant material; the plant source referred to four different hybrids of *Cymbidium* plants, the scientific names of which were not given [4]. No other plant was reported as a source of this compound, and the information on its identity has not been available in the SciFinder database yet. The isolation of **1** from *C. tracyanum* provided the first evidence for a species-defined and wild-type source of cymbisamoquinone.

Compounds **2**–**6** were identified to be 3,7-dihydroxy-2,4,6-trimethoxyphenanthrene [23], tristin [24], gigantol [25], (+)-pinoresinol [26], and calanquinone B [27], respectively. All the compounds have been previously found in other plants of the Orchidaceae family [15,16,23–25,27,28].

The results obtained from the cytotoxicity assay are shown in Table 1. Compounds **2**–**5** did not exert any significant cytotoxic effects on the cancer cells. Furthermore, their IC_{50} values for the normal cell (NIH/3T3) were higher than or very close to those for the cancer cells, indicating their undesirable effects. The compounds showing considerable activity seemed to be the phenanthrenequinones **1** and **6**. Among the isolated compounds, **6** exhibited the strongest and most distinguishable cytotoxic activities on all the tested cells except for MCF-7/DOX cells. Although the compound exerted less potential in killing the cancer cell lines (IC_{50} 11.34 to 45.33 µM) compared to the normal cell line (IC_{50} 2.15 µM), it still demonstrated higher potency than doxorubicin on MCF-7/DOX cells (IC_{50} 11.34 and 19.02 µM for **6** and doxorubicin, respectively). On the other hand, despite no significant cytotoxic activity against almost all the tested cells, **1** demonstrated a noticeable effect against MCF-7/DOX cells. The potency of **1** on these cells (IC_{50} 8.64 µM) was higher than that of the other tested compounds (IC_{50} 11.34 to 70.42 µM), except for mitoxantrone (IC_{50} 0.61 µM). In addition, its activity was relatively selective, being significantly greater than that on the normal cells (IC_{50} 28.49 µM).

Table 1. Cytotoxic activities against cancer and normal cell lines of the tested compounds.

Compound	IC_{50} (μM) *				
	MCF-7	MCF-7/DOX	MCF-7/MX	Caco-2	NIH/3T3
1	43.27 ± 3.91	8.64 ± 0.03	>75	>75	28.49 ± 0.62
2	52.27 ± 1.45	70.42 ± 0.73	66.04 ± 1.04	44.48 ± 0.90	45.51 ± 1.10
3	34.93 ± 1.91	62.78 ± 3.51	70.68 ± 1.19	>75	7.79 ± 0.41
4	52.13 ± 0.11	26.16 ± 0.61	62.13 ± 1.08	>75	4.77 ± 0.40
5	>75	63.91 ± 1.13	>75	>75	16.40 ± 0.21
6	25.97 ± 0.11	11.34 ± 0.83	45.33 ± 1.81	19.16 ± 0.02	2.15 ± 0.11
Doxorubicin	0.81 ± 0.12	19.02 ± 1.35	1.57 ± 0.07	3.09 ± 1.34	5.31 ± 0.59
Mitoxantrone	0.20 ± 1.37	0.61 ± 1.29	10.04 ± 1.54	2.03 ± 1.21	2.06 ± 0.99

*Values are mean ± SD (N = 3).

The SI ($SI^{MCF-7/DOX}$) was found to be 3.30, which was distinguishable among the values calculated for the isolated compounds and comparable to the values for doxorubicin on MCF-7/MX cells and mitoxantrone on MCF-7/DOX cells (Table 2). Compounds **1** and **6** are 1,4-phenanthrenequinones which are closely structurally related. The only difference in their structures, accountable for the different features of their cytotoxic activity in this assay, concerns the substitution at C-3 on the quinone moiety; **6** contains the methoxy group at this position which is missing in the structure of **1**.

Owing to the considerable cytotoxic activity of the MCF-7/DOX cells, the mechanism of **1**-mediated MCF-7/DOX toxicity was evaluated by using molecular docking. A previous study demonstrated that the cytotoxic naphthoquinone rhinacanthin-C was able to induce apoptosis in MCF-7/DOX cells by suppressing the MAPKs; ERK-1/2, JNK and p-38 pathway and Akt/GSK-3β/Nrf-2 pathway which was involved in the regulation of cellular detoxification by antioxidant enzymes (HO-1 and NQO-1) [21]. Both rhinacanthin-C and **1** have the naphthoquinone moiety attached to an aromatic ring. Due to the structural similarity, **1** might be able to inhibit cell survival mechanisms of MAPKs and Akt/GSK-3β/Nrf-2-mediated HO-1 and NQO-1, leading to cell death. Docking results (Table 3) indicated that in the MAPKs pathway, **1** exhibited the strongest interaction with p-38/MAPKs protein as presented by the lowest binding energy and binding inhibition values of −7.17 kcal/mol and 5.5 μM, respectively. The compound also showed strong interaction with JNK/MAPKs protein, whereas the interaction with ERK-2/MAPKs protein was the weakest. These interactions involved various types of bonding; the observed bonds included van der Waals, pi-alkyl, pi-sigma, pi-sulfur, unfavorable acceptor-acceptor, unfavorable bump, carbon-hydrogen, and conventional hydrogen bonds (Fig. 3).

In Akt/GSK-3β/Nrf-2-mediated HO-1 and NQO-1 pathway, the docking study demonstrated that **1** strongly interacted with the upstream Akt/GSK-3β/Nrf-2 signaling pathway but weakly interacted with HO-1 and NQO-1 proteins. The free binding energy and predicted binding inhibition values of **1** with Akt, GSK-3β, and Nrf-2 proteins ranged from −8.01 to −6.45 kcal/mol and 1.34 to 18.71 μM, respectively. Those of **1** with HO-1 and NQO-1 proteins were found to be −5.22 and −5.81 kcal/mol, and 149.39 and 55.09 μM, respectively, referring to low binding affinity action. The amino acid residues of the five proteins formed different types of bonds with **1**, including van der Waals, alkyl, pi-alkyl, pi-anion, pi-cation, pi-sigma, pi-pi stacked, pi-pi T-shaped, carbon-hydrogen, and conventional hydrogen bonds (Figs. 4 and 5).

These findings suggested that **1** displayed a higher binding affinity for inhibition with the MAPKs and upstream

Table 2. SI of the tested compounds.

Compound	SI			
	MCF-7	MCF-7/DOX	MCF-7/MX	Caco-2
1	0.66	3.30	0.38	0.38
2	0.87	0.65	0.69	1.02
3	0.22	0.12	0.11	0.10
4	0.09	0.18	0.08	0.06
5	0.22	0.26	0.22	0.22
6	0.08	0.19	0.05	0.11
Doxorubicin	6.56	0.28	3.38	1.72
Mitoxantrone	10.30	3.38	0.21	1.01

Table 3. Free binding energy and predicted binding inhibition for interactions between **1** and target proteins.

Target protein	Free binding energy (kcal/mol)	Predicted binding inhibition (μM)
MAPKs pathway		
ERK-2	−6.18	29.67
JNK	−7.03	7.05
p-38	−7.17	5.55
Akt/GSK-3β/Nrf-2 pathway		
Akt	−8.01	1.34
GSK-3β	−6.45	18.71
Nrf-2	−7.18	5.47
Detoxification proteins		
HO-1	−5.22	149.39
NQO-1	−5.81	55.09

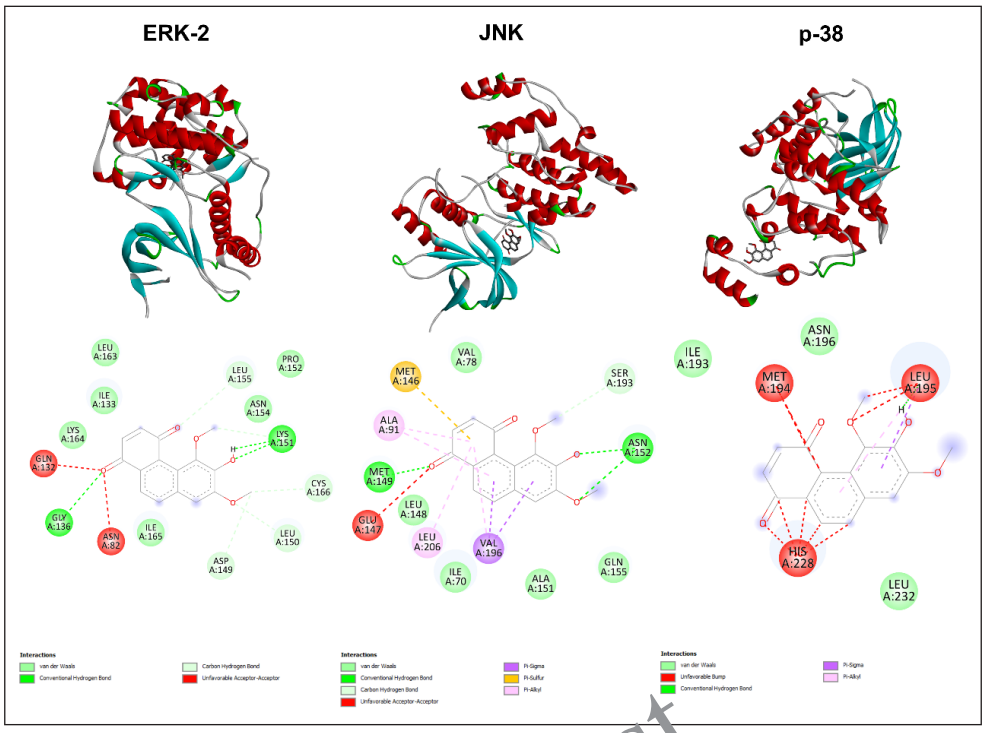

Figure 3. The 2-D and 3-D intermolecular interactions between **1** and ERK-2, JNK and p-38/MAPKs proteins.

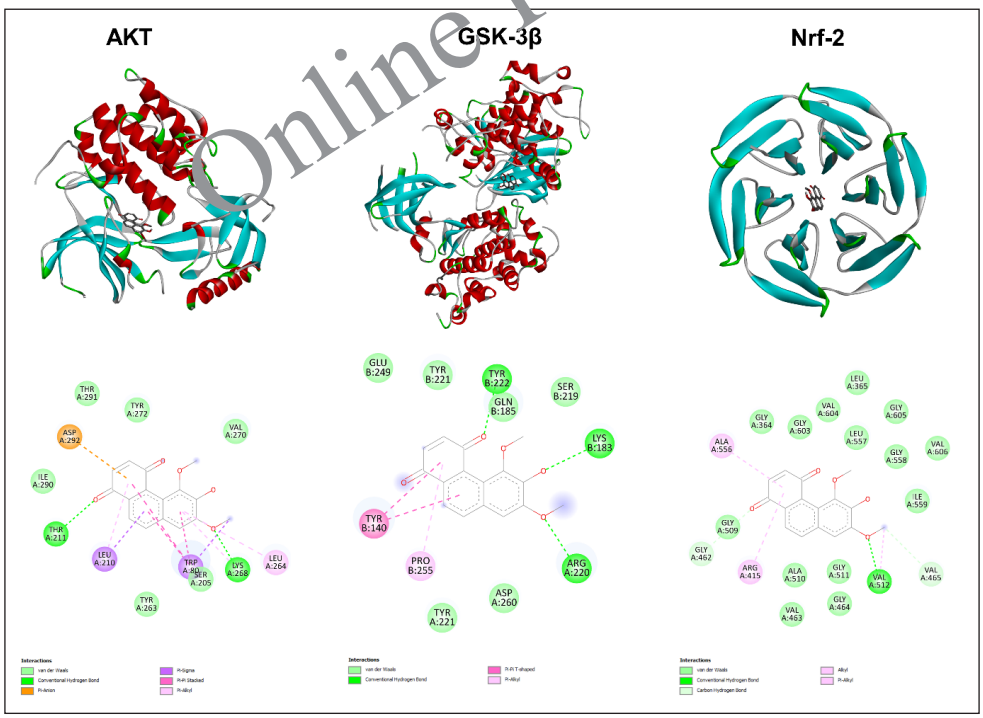

Figure 4. The 2-D and 3-D intermolecular interactions between **1** and Akt/GSK3β/Nrf-2 proteins.

Akt/GSK-3β/Nrf-2 signaling pathways than the downstream mechanism involving the cellular detoxification proteins, HO-1 and NQO-1. It is possible that the cytotoxic activity of **1** against MCF-7/DOX cells involved apoptotic induction via suppression of the cell survival systems mediated by the MAPKs and Akt/GSK-3β/Nrf2 signaling pathways. This hypothetical mechanism of action of **1** should be further confirmed by *in vitro* and *in vivo* studies.

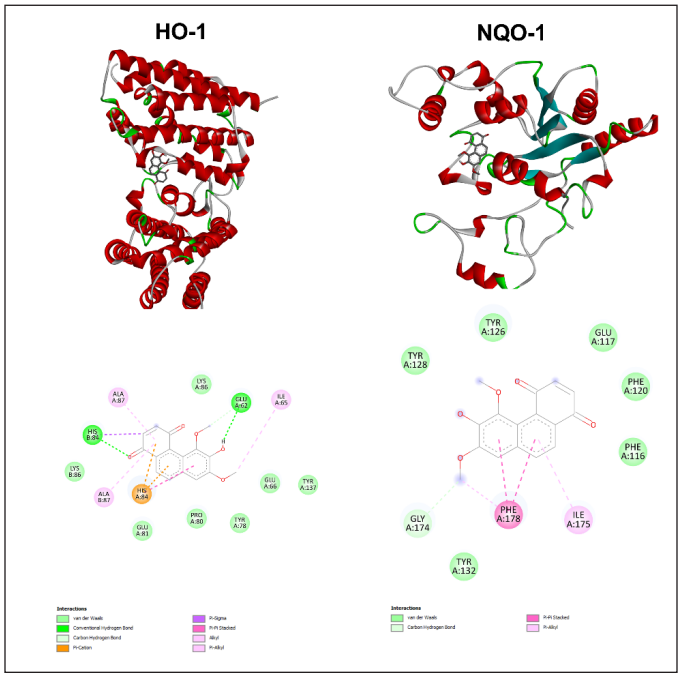

Figure 5. The 2-D and 3-D intermolecular interactions between **1** and NQO-1/HO-1 proteins.

CONCLUSION

The present study provided the first report on phytochemical constituents of *C. tracyanum* L.Castle which included cymbisamoquinone (**1**), calanquinone B (**6**), 3,7-dihydroxy-2,4,6-trimethoxyphenanthrene (**2**), trisin (**3**), gigantol (**4**), and (+)-pinoresinol (**5**). Among the isolated compounds, **1** showed the strongest and relatively selective cytotoxic activity against MCF-7/DOX cells in the MTT assay. Based on the results obtained from the molecular docking study, the cytotoxic activity of **1** on these cells was possibly due to induction of apoptosis via suppression of the cell survival systems mediated by the MAPKs and Akt/GSK-3β/Nrf2 signaling pathways.

ACKNOWLEDGMENT

The authors would like to acknowledge the Pharmaceutical Research Instrument Center, Faculty of Pharmaceutical Sciences, Chulalongkorn University, for providing instrumental facilities in conducting this research work.

AUTHOR CONTRIBUTIONS

NL, CB, and WT substantial contributions to the conception and design, acquisition of data; NL, RS, KLS, SJ, CB, and WT contributed to the interpretation of data and took part in drafting the article or revising it critically for important intellectual content; agreed to submit to the current journal; gave final approval of the version to be published; and agree to be accountable for all aspects of the work. All the authors are eligible to be an author as per the International Committee of Medical Journal Editors (ICMJEs) requirements/guidelines.

FINANCIAL SUPPORT

There is no funding to report.

CONFLICTS OF INTEREST

The authors declare no conflicts of interest.

ETHICAL APPROVALS

This study does not involve experiments on animals or human subjects.

DATA AVAILABILITY

All data generated and analyzed are included in this research article.

PUBLISHER'S NOTE

This journal remains neutral with regard to jurisdictional claims in published institutional affiliation.

REFERENCES

1. Zhang GQ, Chen GZ, Chen LJ, Zhai JW, Huang J, Wu XY, *et al*. Phylogenetic incongruence in *Cymbidium* orchids. Plant Divers. 2021;43(6):452–61. doi: https://doi.org/10.1016/j.pld.2021.08.002
2. Chen SC, Liu ZJ, Zhu GH, Lang KY, Ji ZH, Luo YB, *et al*. Orchidaceae. In: Zhengyi W, Raven PH, Deyuan H, editors. Flora of China. Vol. 25. Beijing, China: Science Press; 2009. pp 260–80.
3. Pal R, Meena NK, Pant RP, Dayamma M. Cymbidium: botany, production, and uses. In: Merillon JM, Kodja H, editors. Orchids phytochemistry, biology and horticulture. New York, NY: Springer; 2020. pp 261–97. doi: https://doi.org/10.1007/978-3-030-11257-8_8-1
4. Axiotis E, Angelis A, Antoniadi L, Petrakis EA, Skaltsounis LA. Phytochemical analysis and dermo-cosmetic evaluation of *Cymbidium* sp. (Orchidaceae) cultivation by-products. Antioxidants. 2022;11(1):101. doi: https://doi.org/10.3390/antiox11010101
5. Jimoh TO, Costa BC, Chansriniyom C, Chaotham C, Chanvorachote P, Rojsitthisak P, *et al*. Three new dihydrophenanthrene derivatives from *Cymbidium ensifolium* and their cytotoxicity against cancer cells. Molecules. 2022;27(7):2222. doi: https://doi.org/10.3390/molecules27072222
6. Lv SS, Fu Y, Chen J, Jiao Y, Chen SQ. Six phenanthrenes from the roots of *Cymbidium faberi* Rolfe. and their biological activities. Nat Prod Res. 2022;36(5):1170–81. doi: https://doi.org/10.1080/14786419.2020.1862836
7. Lertnitikul N, Pattamadilok C, Chansriniyom C, Suttisri R. A new dihydrophenanthrene from *Cymbidium finlaysonianum* and structure revision of cymbinodin-A. J Asian Nat Prod Res. 2020;22(1):083–90. doi: https://doi.org/10.1080/10286020.2018.1540605
8. Yoneyama T, Iseki K, Baba C, Kitagawa Y, Yoshikawa K, Kawano S, *et al*. Phenanthrenes with potent antitrypanosomal activity from roots of *Cymbidium* great flower 'Marylaurencin'. J Stage. 2020;74(2):106–7. doi: https://doi.org/10.24684/jspharm.74.2_106
9. Yoshikawa K, Baba C, Iseki K, Ito T, Asakawa Y, Kawano S, *et al*. Phenanthrene and phenylpropanoid constituents from the roots of *Cymbidium* great flower 'Marylaurencin' and their antimicrobial activity. J Nat Med. 2014;68(4):743–7. doi: https://doi.org/10.1007/s11418-014-0854-8
10. Yoshikawa K, Ito T, Iseki K, Baba C, Imagawa H, Yagi Y, *et al*. Phenanthrene derivatives from *Cymbidium* great flower Marie Laurencin and their biological activities. J Nat Prod. 2012;75(4):605–9. doi: https://doi.org/10.1021/np200788u
11. Majumder PL, Sen RC. Pendulin, a polyoxygenated phenanthrene derivative from the orchid *Cymbidium pendulum*. Phytochemistry.

1991;30(7):2432–4. doi: https://doi.org/10.1016/0031-9422(91)83675-B
12. Barua AK, Ghosh BB, Ray S, Patra A. Cymbinodin-A, a phenanthraquinone from *Cymbidium aloifolium*. Phytochemistry. 1990;29(9):3046–7. doi: https://doi.org/10.1016/0031-9422(90)87138-K
13. Juneja RK, Sharma SC, Tandon JS. Two substituted bibenzyls and a dihydrophenanthrene from *Cymbidium aloifolium*. Phytochemistry. 1987;26(4):1123–5. doi: https://doi.org/10.1080/10286020.2018.1540605
14. Juneja RK, Sharma SC, Tandon JS. A substituted 1,2-diarylethane from *Cymbidium giganteum*. Phytochemistry. 1985;24(2):321–4. doi: https://doi.org/10.1016/S0031-9422(00)83544-X
15. Toth B, Hohmann J, Vasas A. Phenanthrenes: a promising group of plant secondary metabolites. J Nat Prod. 2018;81(3):661–78. doi: https://doi.org/10.1021/acs.jnatprod.7b00619
16. Sut S, Maggi F, Dall'Acqua S. Bioactive secondary metabolites from orchids (Orchidaceae). Chem Biodivers. 2017;14(11):e1700172. doi: https://doi.org/10.1002/cbdv.201700172
17. Kovacs A, Vasas A, Hohmann J. Natural phenanthrenes and their biological activity. Phytochemistry. 2008;69(5):1084–110. doi: https://doi.org/10.1016/j.phytochem.2007.12.005
18. He L, Su Q, Bai L, Li M, Liu J, Liu X, *et al*. Recent research progress on natural small molecule bibenzyls and its derivatives in *Dendrobium* species. Eur J Med Chem. 2020;204(15):112530. doi: https://doi.org/10.1016/j.ejmech.2020.112530
19. Chaisit T, Siripong P, Jianmongkol S. Rhinacanthin-C enhances doxorubicin cytotoxicity via inhibiting the functions of P-glycoprotein and MRP2 in breast cancer cells. Eur J Pharmacol. 2017;795:50–7. doi: https://doi.org/10.1016/j.ejphar.2016.12.002
20. Wongsakul A, Lertnitikul N, Suttisri R, Jianmongkol S. N-Trans-p-coumaroyltyramine enhances indomethacin- and diclofenac-induced apoptosis through endoplasmic reticulum stress-dependent mechanism in MCF-7 cells. Anticancer Res. 2022;42(4):1831–41. doi: https://doi.org/10.21873/anticanres.15659.
21. Chaisit S, Jianmongkol S. Apoptosis inducing activity of rhinacanthin-C in doxorubicin-resistant breast cancer MCF-7 cells. Biol Pharm Bull. 2021;44(9):1239–46. doi: https://doi.org/ 10.1248/bpb.b21-00015
22. Ramirez D, Caballero J. Is it reliable to take the molecular docking top scoring position as the best solution without considering available structural data? Molecules. 2018;23(5):1038. doi: https://doi.org/10.3390/molecules23051038
23. Chen YG, Xu JJ, Yu H, Chen Q, Zhang YL, Liu Y, *et al*. 3,7-Dihydroxy-2,4,6-trimethoxyphenanthrene, a new phenanthrene from *Bulbophyllum odoratissimum*. J Korean Chem Soc. 2007;51(4):352–5. doi: https://doi.org/10.5012/jkcs.2007.51.4.352
24. Bhinija K, Huehne PS, Prawat H, Ruchirawat S, Saimanee B, Mongkolsuk S, *et al*. The rhizome of *Bulbophyllum* orchid is the rich source of cytotoxic bioactive compounds, the potential anticancer agent. S Afr J Bot. 2021;141:367–72. doi: https://doi.org/10.1016/j.sajb.2021.05.013
25. Chen YG, Yu H, Lian X. Isolation of stilbenoids and lignans from *Dendrobium hongdie*. Trop J Pharm Res. 2015;14(11):2055–9. doi: https://doi.org/10.4314/TJPR.V14I11.15
26. Ragasa CY, Tan MCS, Fortin DR, Shen CC. Chemical constituents of *Ixora philippinensis* Merr. J Appl Pharm Sci. 2015;5(9):062–7. doi: https://doi.org/10.7324/JAPS.2015.50912
27. Lee CL, Chang FR, Yen MH, Yu D, Liu YN, Bastow KF, *et al*. Cytotoxic phenanthrenequinones and 9,10-dihydrophenanthrenes from *Calanthe arisanensis*. J Nat Prod. 2009;72(2):210–3. doi: https://doi.org/10.1021/np800622a
28. Wang YH. Traditional uses and pharmacologically active constituents of *Dendrobium* plants for dermatological disorders: a review. Nat Prod Bioprospect. 2021;11(5):465–87. doi: https://doi.org/10.1007/s13659-021-00305-0

How to cite this article:
Lertnitikul N, Suttisri R, Sein KL, Jianmongkol S, Boonyong C, Thanakijcharoenpath W. Cytotoxic constituents of *Cymbidium tracyanum* L.Castle. J Appl Pharm Sci. 2024. http://doi.org/10.7324/JAPS.2024.158840